HEPATOLOGY

AASLD
AMERICAN ASSOCIATION FOR
THE STUDY OF LIVER DISEASES

HEPATOLOGY, VOL. 68, NO. 2, 2018

LIVER BIOLOGY/PATHOBIOLOGY

Angiocrine Wnt Signaling Controls Liver Growth and Metabolic Maturation in Mice

Thomas Leibing [iD],[1]* Cyrill Géraud,[1]* Iris Augustin,[2,3] Michael Boutros,[2] Hellmut G. Augustin,[4,5] Jürgen G. Okun,[6] Claus-Dieter Langhans,[6] Johanna Zierow,[1] Sebastian A. Wohlfeil,[1] Victor Olsavszky,[1] Kai Schledzewski,[1] Sergij Goerdt,[1,7] and Philipp-Sebastian Koch[1]

Postnatal liver development is characterized by hepatocyte growth, proliferation, and functional maturation. Notably, canonical Wnt signaling in hepatocytes has been identified as an important regulator of final adult liver size and metabolic liver zonation. The cellular origin of Wnt ligands responsible for homeostatic liver/body weight ratio (LW/BW) remained unclear, which was also attributable to a lack of suitable endothelial Cre driver mice. To comprehensively analyze the effects of hepatic angiocrine Wnt signaling on liver development and metabolic functions, we used endothelial subtype-specific Stab2-Cre driver mice to delete Wls from hepatic endothelial cells (HECs). The resultant Stab2-Cre$^{tg/wt}$;Wls$^{fl/fl}$ (Wls-HECKO) mice were viable, but showed a significantly reduced LW/BW. Specifically, ablation of angiocrine Wnt signaling impaired metabolic zonation in the liver, as shown by loss of pericentral, β-catenin-dependent target genes such as glutamine synthase (Glul), RhBg, Axin2, and cytochrome P450 2E1, as well as by extended expression of periportal genes such as arginase 1. Furthermore, endothelial subtype-specific expression of a c-terminally YFP-tagged Wls fusion protein in Wls-HECKO mice (Stab2-Cre$^{tg/wt}$;Wls$^{fl/fl}$; Rosa26:Wls-YFP$^{fl/wt}$ [Wls-rescue]) restored metabolic liver zonation. Interestingly, lipid metabolism was altered in Wls-HECKO mice exhibiting significantly reduced plasma cholesterol levels, while maintaining normal plasma triglyceride and blood glucose concentrations. On the contrary, zonal expression of Endomucin, LYVE1, and other markers of HEC heterogeneity were not altered in Wls-HECKO livers. *Conclusion:* Angiocrine Wnt signaling controls liver growth as well as development of metabolic liver zonation in mice, whereas intrahepatic HEC zonation is not affected. (HEPATOLOGY 2018; 68:707-722).

Liver sinusoidal endothelial cells (LSECs) are morphologically unique and functionally specialized microvascular endothelial cells (ECs). In contrast to most other ECs, LSECs are discontinuous ECs, lack a basement membrane, and are highly permeable microvessels with specialized intercellular

junctions.[1] Recently, we identified transcription factor GATA4 as a master regulator of hepatic microvascular specification.[2] Using their unique molecular repertoire, LSECs contribute to clearance of noxious molecules from the peripheral blood by scavenger receptors such as Stabilin (Stab) 1 and Stab2,[3] present antigens, induce immune tolerance,[4] and regulate blood flow and nutrient concentration in the space of Disse.[5] Moreover, LSECs display heterogeneous morphological features and molecular properties dependent on their localization in the hepatic lobule, with high Endomucin (EMCN) expression in pericentral LSECs and central vein endothelial cells (CVECs)[6] and strong LYVE1 expression in midzonal LSECs.[7]

LSECs do not only act as scavenger endothelial cells with a high permeability for cells and solutes, but also play a key role in liver diseases and regeneration through angiocrine signaling.[8] Recently, we have identified bone morphogenetic protein (Bmp) 2 as an LSEC-derived angiokine controlling iron homeostasis in mice. In this connection, angiocrine Bmp2 signaling acts together with angiocrine Bmp6 signaling in a nonredundant manner.[9,10] Moreover, previous results demonstrated that, among others, angiopoietin-2,[11] Wnt2,[8,12] Wnt9b,[13] and hepatocyte growth factor[8,12] function as LSEC-derived angiokines. HECs not only express Wnt ligands Wnt2b and Wnt9b, but also Wnt cargo receptor Evi (Wls),[14,15] a transmembrane protein indispensable for the exocytosis of Wnt ligands.[16]

Canonical Wnt signaling-dependent hepatocyte (HC) heterogeneity in the hepatic lobule[17,18] is generally referred to as metabolic liver zonation.[19,20]

Using conditional null mice for Wls, it was shown that neither HC- nor Kupffer cell (KC)-derived Wnt ligands could induce β-catenin activation in HCs.[21] Under wild-type (WT) conditions, HCs in proximity to the central vein (pericentral HCs) show transcriptionally active β-catenin[17,18,22] and express enzymes involved in xenobiotic metabolism, glycolysis, and glutamine synthesis.[20] Similarly, β-catenin target genes, like glutamine synthetase (Glul) and Axin2,[13] are exclusively expressed in pericentral HCs. Cell division of diploid Axin2 and Glul expressing HCs, which are located adjacent to the central vein, has been suggested to maintain homeostatic renewal of the liver.[13] CVECs express Wnt2, Wnt9b,[13] and R-spondin 3 (RSPO3)[23]; high transcriptional activity of β-catenin in pericentral HCs is mediated through paracrine Wnt ligands and the RSPO–LGR4/5–ZNRF3/RNF43 module.[23,24] RNA *in situ* hybridization as well as qRT-PCR analysis of sorted ECs indicated that LSECs produce Wnt2 as well,[13] which is in line with previous work by us and others.[14,15] HC-specific (Alb-Cre) β-catenin knockout (KO; Ctnnb1$^{fl/fl}$; Alb-Cre$^{tg/wt}$)[17], Alb-Cre LRP5/6 KO (Lrp5$^{fl/fl}$; Lrp6$^{fl/fl}$; Alb-Cre$^{tg/wt}$)[21], and Alb-Cre LGR4/5 KO (Lgr4$^{fl/fl}$; Lgr5$^{fl/fl}$; Alb-Cre$^{tg/wt}$)[24] mice display a reduced liver/body weight ratio (LW/BW) and lack the expression of pericentral β-catenin target genes (Glul, Axin2), but express periportal proteins in the whole-liver lobule instead. Periportal HCs, close to the portal fields, perform functions such as amino and fatty acid degradation, gluconeogenesis, and cholesterol synthesis.[22,25] In contrast to pericentral HCs, arginase 1 (Arg1)

ARTICLE INFORMATION:

From the [1]Department of Dermatology, Venereology, and Allergology, University Medical Center and Medical Faculty Mannheim, Heidelberg University, and Center of Excellence in Dermatology, Mannheim, Germany; [2]German Cancer Research Center (DKFZ), Division of Signaling and Functional Genomics and Heidelberg University, Faculty of Medicine Mannheim, Department of Cell and Molecular Biology, Heidelberg, Germany; [3]Molecular Cell Biology and Plant Cell Technology, University of Applied Sciences Weihenstephan-Triesdorf, Freising, Germany; [4]Division of Vascular Oncology and Metastasis (DKFZ-ZMBH Alliance), DKFZ, Heidelberg, Germany; [5]Department of Vascular Biology and Tumor Angiogenesis (CBTM), Medical Faculty Mannheim, Heidelberg University, Mannheim, Germany; [6]Department of General Pediatrics, Division of Inherited Metabolic Diseases, University Children's Hospital, Heidelberg, Germany; and [7]European Center for Angioscience, Medical Faculty Mannheim, University of Heidelberg, Mannheim, Germany.

ADDRESS CORRESPONDENCE AND REPRINT REQUESTS TO:

Philipp-Sebastian Koch, M.D.
Department of Dermatology, Venereology and Allergology,
University Medical Center Mannheim, Heidelberg University
Theodor-Kutzer-Ufer 1-3
D-68165 Mannheim, Germany
E-mail: philipp.koch@umm.de
Tel: +49 (0) 621 383 2280; or

Cyrill Géraud, M.D.
Department of Dermatology, Venereology and Allergology,
University Medical Center Mannheim, Heidelberg University
Theodor-Kutzer-Ufer 1-3
D-68165 Mannheim, Germany
E-mail: cyrill.geraud@umm.de
Tel: +49 (0) 621 383 2280

expression is limited to periportal and midlobular HCs, whereas Glul is missing.[20]

Abrogating Wnt signaling from HECs using conditional Wls null mice generated by inducible VE-cadherin Cre-ERT2 driver mice has been reported to result in a partial endothelial Wls deficiency in the liver, leading to a decrease in Axin2 as well as Glul mRNA in pericentral HCs.[13] In order to comprehensively analyze the effects of hepatic angiocrine Wnt signaling on liver development and metabolic functions, we used endothelial subtype-specific Stab2-Cre driver mice to delete Wls from HECs. To this end, Stab2-Cre[tg/wt];Wls^{fl/fl} (Wls-HECKO) mice showed that Wnt ligands secreted by liver endothelium controlled liver growth as measured by LW/BW as well as establishment of metabolic liver zonation, although LSEC zonation remained unchanged.

Materials and Methods

GENERATION OF TRANSGENIC MICE

Stabilin-2[tg1.2cre] transgenic founder mice (Stab2-Cre[tg/wt]) were generated and characterized by crossing to Rosa26:eYFP^{fl/fl} (B6.129X1-Gt(ROSA) 26Sor[tm1(EYFP)Cos]/J; [JAX 006148][26]) reporter animals as described.[2,9] Stab2-Cre[tg/wt] mice were crossed to a mouse line bearing floxed alleles of Wls [B6-Gpr177[tm1 1775.302Arte]; TaconicArtemis] (Wls^{fl/fl}).[27] To obtain loss-of-function (Stab2-Cre[tg/wt];Wls^{fl/fl} (Wls-HECKO)) and control (Ctrl; Stab2-Cre[wt/wt]; Wls[fl/wt] and Stab2-Cre[wt/wt];Wls^{fl/fl}) genotypes, the resulting F1 offspring (Stab2-Cre[tg/wt];Wls[fl/wt]) was crossed to Wls^{fl/fl} mice. Additionally, Rosa26:Wls-YFP^{fl/fl} mice (Gt(ROSA)26Sortm1.1(Wls/YFP)-Mbtr[28]) were crossed with Wls^{fl/fl} mice to generate Stab2-Cre[tg/wt];Wls^{fl/fl};Rosa26:Wls-YFP[fl/wt] (Wls-rescue) genotypes; Stab2-Cre[tg/wt];Wls^{fl/fl};Rosa26:eYFP[fl/wt] (Wls-HECKO;eYFP) were used as controls. Stab2-Cre[tg/wt];Rosa26:eYFP[fl/wt] animals (eYFP-reporter) were used to study enhanced yellow fluorescent protein (eYFP) expression at different time points in development. Genotyping was performed at postnatal day (P) 28 using primer pairs PC1 and PC2 for Cre, PW1 and PW2 for Wls, PY1, PY2, and PY3 for Rosa26:eYFP, and PRE1, PRE2, and PRE3 for Rosa26:Wls-YFP (Supporting Table S1). All animals used were on a C57BL/6 background.

ANIMAL EXPERIMENTS

Mice used were between 11 and 14 weeks of age; sibling controls were used except for Wls-rescue, for which background, age- and sex-matched controls from the same facility were used. eYFP-reporter animals were sacrificed at embryonic day (E)11.5 and 6 weeks. All animals were hosted in single ventilated cages (Sealsafe plus DGM [Techniplast, Italy] and Bedding H0234-20 [Ssniff, Germany]) in a 12-hour day/night cycle under specific pathogen-free (SPF) conditions and fed *ad libitum* with a standard rodent diet (ssniffR/M-H autoclavable, V1534-000; Ssniff). Bisected kidney basins were used as enrichment. All animal experiments were approved by the animal ethics committee in Baden-Wuerttemberg (Regierungspraesidium Karlsruhe).

BLOOD PARAMETERS

Blood samples were taken from the *Vena facialis* after 4 hours of fasting during the day cycle. Blood sugar was measured using a point-of-care testing device (Stat-StripXpress; Nova Biomedical, Waltham, MA, USA). Plasma was separated (centrifugation at 2,000g for 5 minutes at 20°C in Microvette 500 LH; Sarstedt, Germany) and analyzed for triglycerides, cholesterol, bilirubin, alanine aminotransferase (ALT), aspartate aminotransferase (AST), glutamate dehydrogenase (GLDH), cholinesterase, and total protein (cobas c 311 Analyser; F. Hoffmann-La Roche AG, Switzerland). Calibration and independent controls were used as recommended by the manufacturer. Plasma was diluted 1:5, and total bile acid content was measured using a colorimetric total bile acid assay kit (STA-631; Cell Biolabs, San Diego, CA, USA) according to the manufacturer's instructions. Bile acid measurements were performed in duplicates. For sterol (except cholesterol) quantification, plasma was hydrolyzed and extracted as described.[29] Subsequent differentiation and quantification of sterols were performed by gas chromatography/mass spectrometry (GC/MS).[30]

MEASUREMENT OF HEPATIC CHOLESTEROL/STEROLE AND BILE ACID LEVELS

Dissected wet liver was homogenized in ddH$_2$O (Precellys Evolution [EQ02520-300-RD000.0] with Precellys ceramic kit 1.4/2.8 mm 2 mL tubes [91-PCS-CKM]; Bertin Technologies S.A.S., Montigny Le Bretonneux, France) for 3 × 15 seconds

at 5,000 rpm. Total bile acid content in lysates was measured using a colorimetric total bile acid assay kit (STA-631; Cell Biolabs) according to the manufacturer's instructions. Bile acid measurements were performed in duplicates. For cholesterol/sterole measurement, liver lysates were hydrolyzed and extracted as described.[29] Subsequent differentiation and quantification of cholesterol/sterols was performed by GC/MC.[30] Measured bile acid and cholesterol/sterole contents were normalized to protein content in homogenates, as determinded by the method of Lowry with the modifications of Helenius and Simons,[31] using bovine serum albumin as a standard.

ELECTROSPRAY IONIZATION/ TANDEM MS–BASED ACYLCARNITINE PROFILING IN DRIED BLOOD

Determination of acylcarnitines as markers for mitochondrial fatty acid oxidation was performed by electrospray ionization/tandem MS[32,33] in dried blood spots (samples obtained from the *V. facialis* after 4 hours of fasting during day cycle) according to Okun et al.[34]

TRANSMISSION ELECTRON MICROSCOPY

Liver from perfusion-fixed Wls-HECKO mice was resin-embedded according to standard procedures. In brief, preflush of anesthetized animals with Sorenson buffer was followed by perfusion and subsequent immersion with freshly prepared aldehyde fixative (4% formaldehyde, 2% glutaraldehyde, 1 mM of $MgCl_2$, and 1 mM $CaCl_2$ in 100 mM of Na-cacodylate; pH 7.2). Vibratome sections (200 μm thick) of the liver were prepared and postfixed with either 1% osmium-tetroxide or osmium-ferrocyanide (i.e., 1% OsO_4/1.3% $K_4Fe(CN)_6$), dehydrated with ethanol, and embedded in epoxy resin. Ultrathin sections (60 nm) poststained with uranyl and lead were observed in a Zeiss EM 910 at 100 kV (Carl Zeiss, Oberkochen, Germany), and micrographs were taken with image plates scanned at 15-μm resolution (Ditabis, Pforzheim, Germany).

LIVER DISSECTION, CRYOPRESERVATION, AND PARAFFIN EMBEDDING

Mice were sacrificed by cervical dislocation. Tail clipping was performed for genotype reconfirmation. Livers

were fixed in 4% paraformaldehyde (PFA) at 4°C for 24 hours, followed by paraffin embedding according to standard protocols. For (e)YFP co-immunofluorescence (Co-IF) staining, liver slices were embedded in optimum cutting temperature (OCT) compound (Sakura Finetek Europe B.V. KvK, Netherlands) after incubation for 24 hours in 4% PFA followed by 24-hour incubation in 30% sucrose in phosphate-buffered saline (PBS). For Stab1, Stab2, and Oil Red O stainings, liver slices were fresh frozen in OCT (Sakura).

EMBRYO DISSECTION, GENOTYPING, AND EMBEDDING

Pregnant mice were sacrificed by cervical dislocation. Embryos were dissected and genotyping was performed from the collected yolk sac tissue. Embryos were fixed in 4% PFA at 4°C for 24 hours, followed by 24-hour 30% sucrose treatment. Following fixation, embryos were embedded in OCT (Sakura).

IMMUNOHISTOCHEMISTRY AND IMMUNOFLURESCENCE

Paraffin sections (1-5 μm) were deparaffinized and rehydrated according to standard protocols. Antigen retrieval was carried out with Epitope Retrieval solution (Novocastra, Leica Microsystems, Germany) at either pH 6 or pH 8. For (e)YFP Co-IF, PFA-fixed cryosections (8 μm) were rehydrated in PBS. First antibody was incubated over night at 4°C; secondary antibody was incubated 1 hour at room temperature after three washing steps with PBS. Sections were mounted with Dako fluorescent mounting medium (Dako, Agilent Technologies, Santa Clara, CA, USA). Paraffin sections were stained as described.[3] For hematoxylin and eosin (H&E), periodic acid Schiff (PAS), Prussian blue, and Sirius red staining, formalin-fixed, paraffin-embedded samples were processed according to standard protocols provided by the manufacturer. Oil Red O staining was performed on 8-μm unfixed liver sections as described.[22]

RNA *IN SITU* HYBRIDIZATION

PFA-fixed liver tissue was sectioned at 4 microns. A modified nonisotopic *in situ* hybridization protocol was carried out using the RNAscope 2.5 HD Red kit (Advanced Cell Diagnostics, Newark, CA, USA) following the manufacturer's recommended protocol, with specific probes against the positive control mouse Ppib

(Cyclophilin B) gene and mouse Axin2. Sections were ultimately stained with 3′-diaminobenzidine and counterstained with hematoxylin.

PRIMARY ECs

LSECs were isolated and purified using CD146 (LSEC) MicroBeads (Miltenyi Biotec GmbH, Germany) as described.[35] Three male mice per group were analyzed. Fluorescence-activated cell sorting–based analysis confirmed purity of LSECs by detection of directly labeled antibodies against Stab2 and CD11b (data not shown).

qRT-PCR

Primers were designed using Primer-Blast (National Center for Biotechnology Information; Supporting Table S1). Total RNA from isolated LSECs was extracted with the EZNA Total-RNA-Kit (OMEGA Bio-tek, Norcross, GA, USA) and reverse transcribed into complementary DNA with RevertAid H-Minus M-MuLV transcriptase (Thermo Fisher Scientific, Waltham, MA, USA). qRT-PCR analysis was performed in the Mx3005P system (Agilent technologies) using SYBR Green PCR Master-Mix (Thermo Fisher Scientific). Data represent mean of at least three biological replicates. Gene expression was normalized to a reference gene (β-Actin) and calculated using the ΔCt (threshold cycle) method. The $\Delta\Delta$Ct method was used to calculate relative fold change between Ctrl and Wls-HECKO.

CONFOCAL MICROSCOPY

Fluorescent-labeled sections were analyzed by a TCS SP5 DS or TCS SP5 MP laser scanning spectral confocal microscope (Leica Microsystems, Germany). Excitation wavelengths were set at 488, 543, and 633 nm. Emission maxima at 518, 570, and 673 nm were detected to visualize Alexa Fluor 488, cyanine 3 (Cy3), and Alexa Fluor 647 conjugates, respectively. Images (three representative areas per sample) were acquired in a sequential mode and processed with Leica confocal software and ImageJ software (National Institutes of Health, Bethesda, MD).

ANTIBODIES

Primary Antibodies

Primary antibodies were rabbit anti-ICAM1 (intracellular adhesion molecule 1; 10020-1-AP; Proteintech, Chicago, IL, USA), rat anti-CD68 (137002; BioLegend, San Diego, CA, USA), goat anti-CD32b (AF1330 and AF1460; R&D Systems, Minneapolis, MN, USA), biotinylated mouse anti-Stabilin-2 clone 3.1 antibody,[3] goat anti-Lyve1 (AF2125; R&D Systems), rat anti-EMCN (eBioV.7C7; Thermo Fisher Scientific), chicken anti–green fluorescent protein (AB13970; Abcam, Cambridge, UK), rabbit anti-Glul (sc-9067; Santa Cruz Biotechnology, Dallas, TX, USA), goat anti-Arginase 1 (Arg1; sc-18351, Santa Cruz Biotechnology), rabbit anti-CYP (cytochrome P450) 2E1 (AB1252; Merck Millipore, Germany), goat anti-RhBg (PA5-19369; Thermo Fisher Scientific), and rabbit anti-β-catenin (AB32572; Abcam).

Secondary Antibodies

Appropriate horseradish peroxidase–, Alexa-Fluor 488–, Alexa-Fluor 647– and Cy3-conjugated secondary antibodies were purchased from Dianova (Germany), GE-Healthcare (United States), and Jackson Immunoresearch (Stratech, UK).

STATISTICAL ANALYSIS

All statistical analyses were performed with JMP software (version 11; SAS Institute Inc., United States). For pair-wise comparisons, the t test was used when normality was proven. For statistical analysis of sampling distributions, Pearson's chi-squared test was used. For statistical analysis of ΔCt values between groups, the Mann-Whitney U test was used. Differences between data sets with $P < 0.05$ were considered statistically significant except for dry blood card sample test and liver/plasma sterole levels, where a Bonferroni correction was applied, resulting in $P < 0.001$ (dry blood cards) and $P < 0.0055$ (sterols) for statistical significance.

Results

GENERATION AND CHARACTERIZATION OF HEPATIC ANGIOCRINE Wnt SIGNALING-DEFICIENT MICE

Endothelial subtype-specific Stab2-Cre driver mice were crossed with floxed Wls mice to delete Wls from HECs. Wls-HECKO mice (Stab2-Cre$^{tg/wt}$;Wls$^{fl/fl}$) were viable, but revealed significantly less female
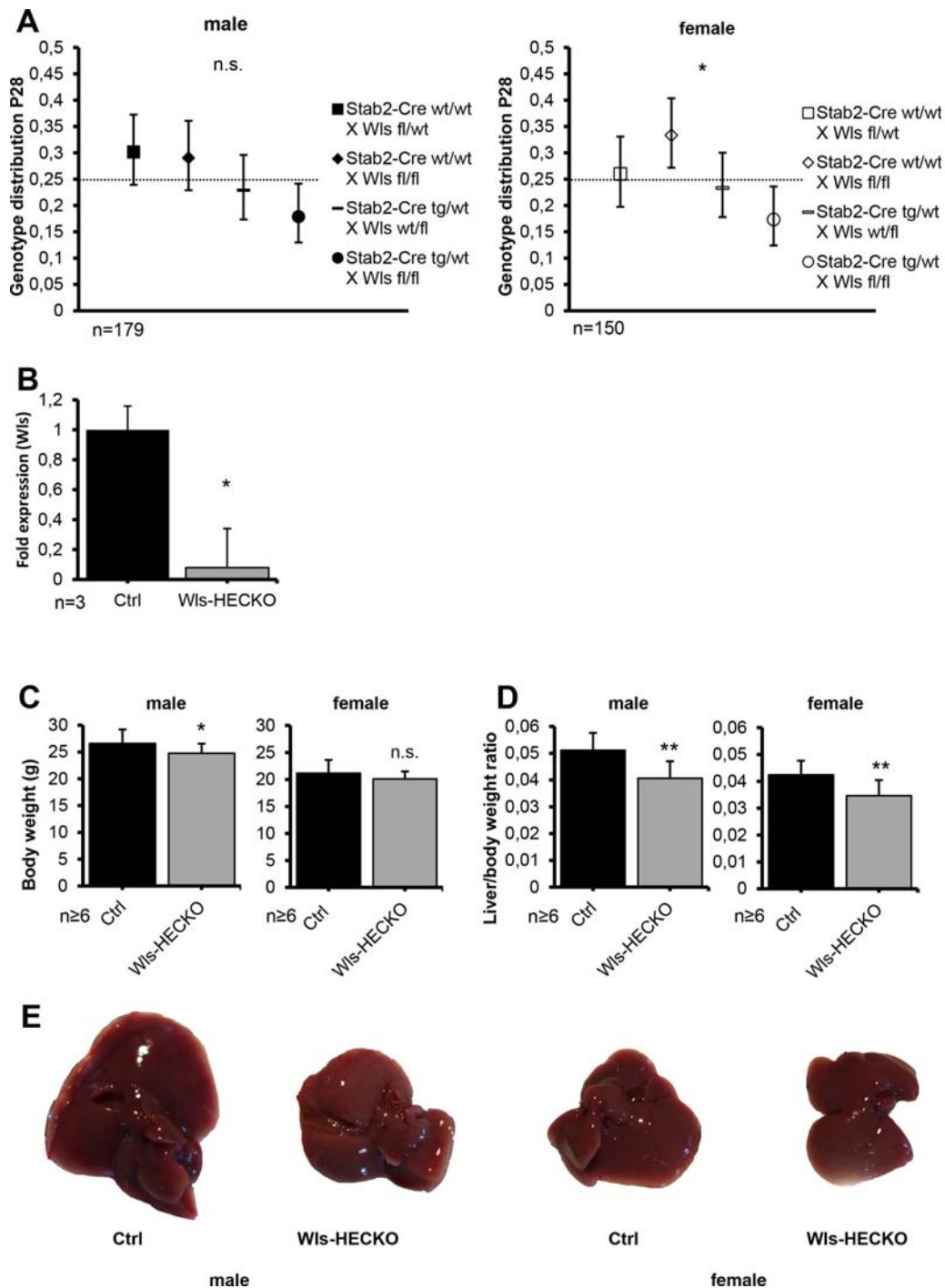
FIG. 1. Wls-HECKO mice are viable and show a reduction of endothelial Wls (*$P < 0.05$; **$P < 0.01$; n.s. = not significant). (A) Genotype distribution of male (left) and female (right) mice at P28 (bars, 95% confidence intervals). (B) Reduction of Wls mRNA in HECs shown by qRT-PCR. Fold change relative to β-Actin is shown; Ctrl was set to 1. Bars represent SEM. Mean fold reduction in Wls-HECKO is 12.5 ($P = 0.0495$; n = 3). Mice used were 12-week-old males. (C) Body weight differs significantly between male Ctrl and male Wls-HECKO mice (26.8 vs. 24.6 g; $P = 0.0132$) at 13 weeks. In female mice, no significance in body weight is found between Ctrl and Wls-HECKO, although there is a trend ($P = 0.0759$) toward a slightly lower body weight. (D) LW/BW at 13 weeks differs significantly between both male Ctrl and male Wls-HECKO (5.1% vs. 4.1%; $P < 0.01$), as well as female Ctrl and female Wls-HECKO (4.2% vs. 3.1%; $P < 0.01$), respectively. (E) Representative pictures of sectioned livers from male (left) and female (right) Ctrl and Wls-HECKO mice (12 weeks old). Abbreviation: P, postnatal day.
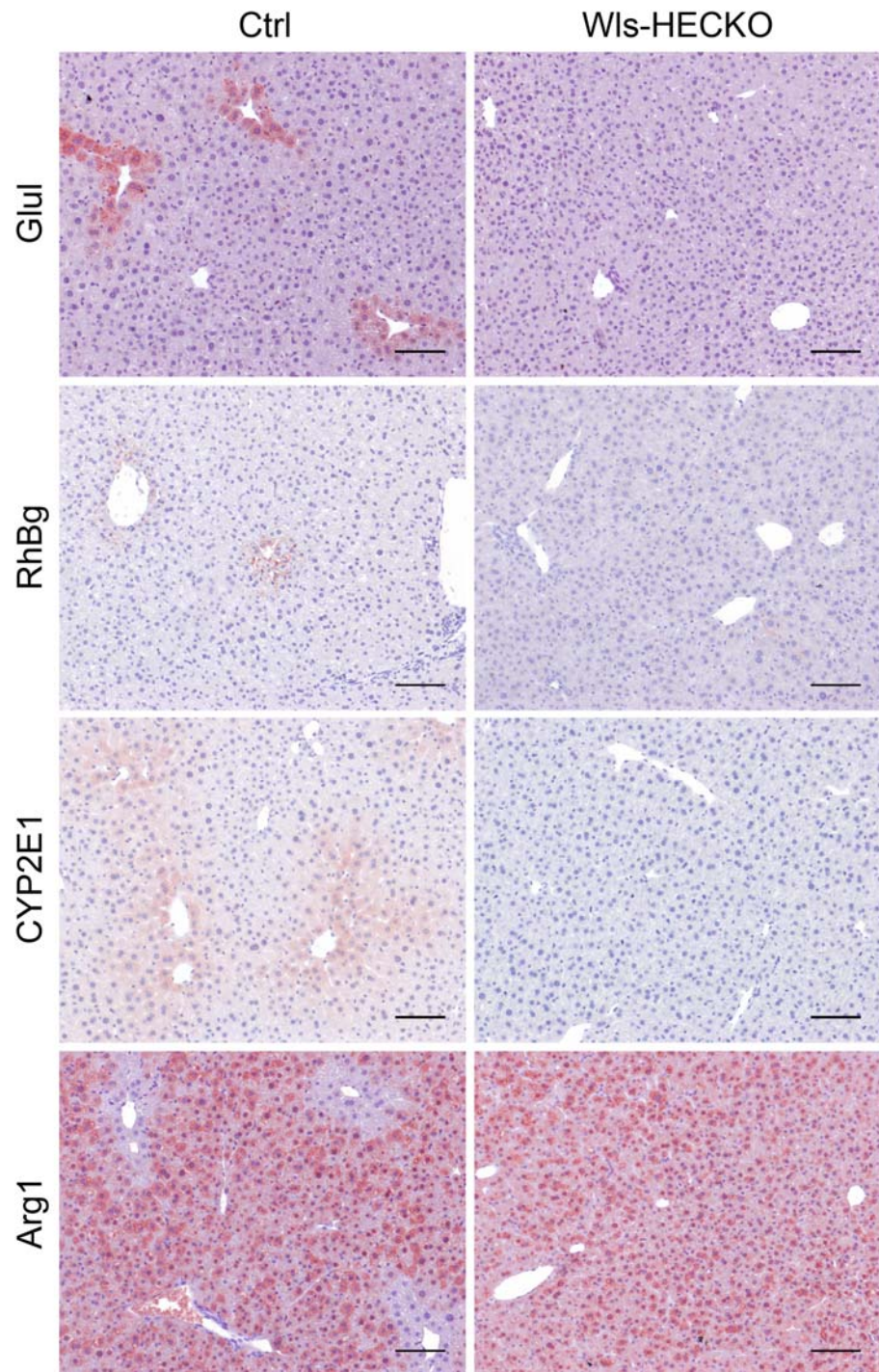
FIG. 2. Disturbed metabolic zonation in Wls-HECKO livers. Immunohisto-chemistry (10× objective) shows Glul, RhBg, Arg1, and CYP2E1 staining pattern in Ctrl pericentral HCs (left) in comparison to Wls-HECKO (right). Scale bar = 100 μm; n = 7.

Wls-HECKO mice ($P = 0.0477$) and a drop in males ($P = 0.0708$) compared to the expected Mendelian ratio (Fig. 1A). Freshly isolated LSECs showed a 12.5-fold reduction of Wls expression in Wls-HECKO HECs compared to control ($P < 0.05$), indicating high penetrance of Wls deficiency in Wls-

HECKO livers (Fig. 1B). Stab2-Cre[tg/wt];Wls^{fl/fl}; Rosa26eYFP[fl/wt] (Wls-HECKO;eYFP) reporter mice showed restriction of eYFP expression to HECs as analyzed by Co-IF with pan-EC marker ICAM1, KC marker CD68, and Emcn, respectively. In addition, all subpopulations of ECs in Wls-HECKO;eYFP livers
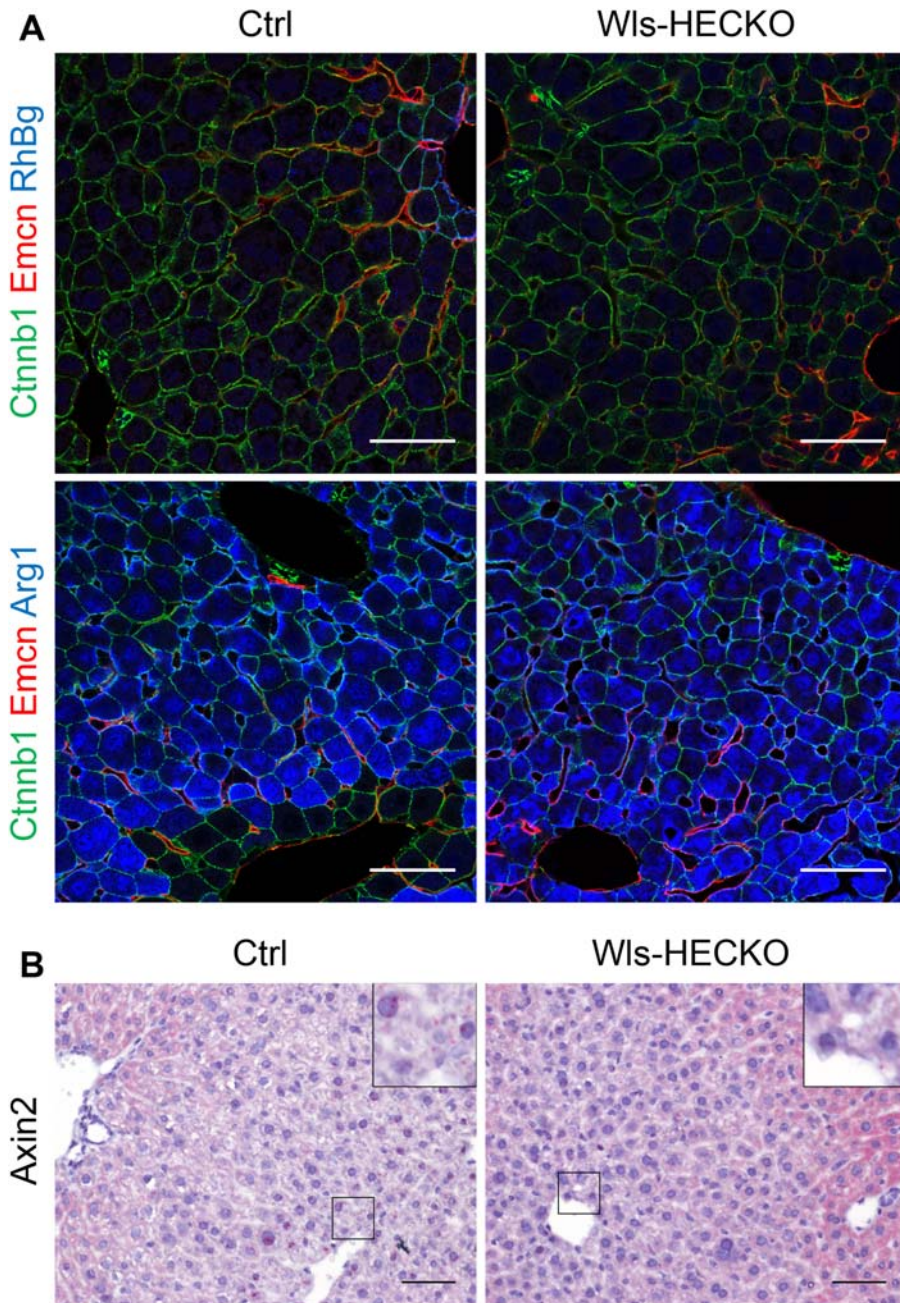
FIG. 3. β-catenin distribution and Axin2 expression in the hepatic lobule. (A) Representative pictures of immunofluorescence (63× objective) showing membranous β-catenin staining in HCs and cholangiocytes and EMCN (red) staining in CVECs and pericentral LSECs in both Ctrl (left) and Wls-HECKO (right). RhBg (blue) is expressed in HCs adjacent to CVECs expressing EMCN in Ctrl (upper left); RhBg is missing in Wls-HECKO (upper right). Arg1 is not expressed in pericentral HCs in Ctrl (blue, lower left), but positive in Wls-HECKO (blue, lower right). Scale bar = 50 μm; n = 5. (B) Axin2 is highly expressed in pericentral HCs in Ctrl; low-level activity in some cells can be seen in Wls-HECKO. 20× objective; Scale bar = 50 μm; n = 3.

(i.e., CVECs, pericentral LSECs, periportal LSECs, portal vein ECs, and hepatic artery ECs) revealed eYFP expression, indicating Cre-mediated Rosa26:eYFP locus activation (Supporting Figs. S1-S3). eYFP expression in eYFP-reporter animals was detectable at both E11.5 and at 6 weeks postnatally, indicating a stable recombination that starts at an early time point during embryonic liver development and persists throughout adulthood (Supporting Fig. S4A,B).

DECREASED LW/BW IN Wls-HECKO MICE

Upon overall inspection, Wls-HECKO could not be distinguished from control animals. However, Wls-HECKO males showed a slightly reduced body weight (24.6 g in Wls-HECKO vs. 26.8 g in control mice; P = 0.0132), whereas the body weight difference of female mice did not

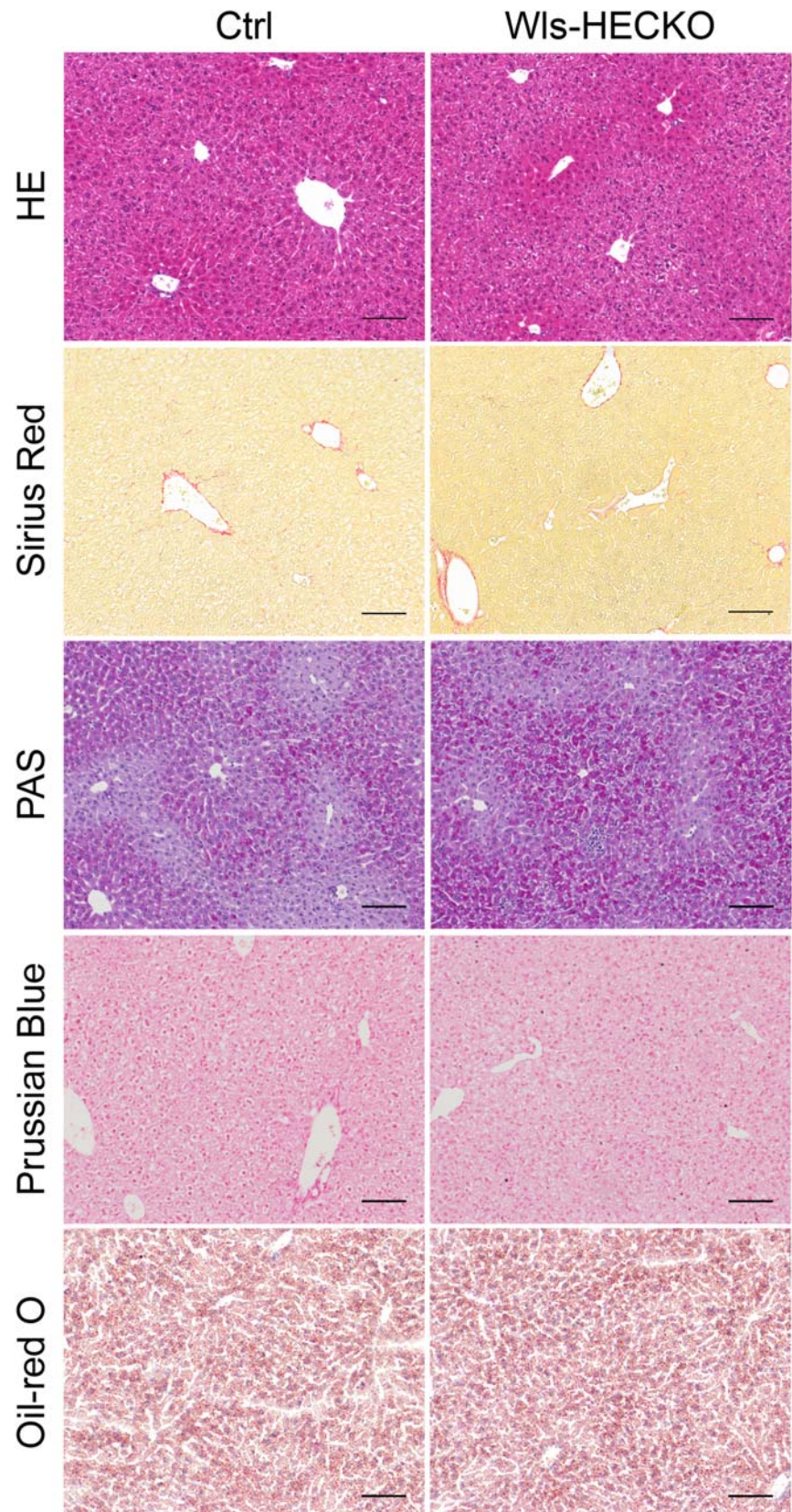**FIG. 4.** No major differences in routine stainings of Wls-HECKO livers. H&E, Sirius Red, PAS, Prussian blue, and Oil Red O staining of Ctrl (left) and Wls-HECKO (right) liver sections (10× objective). PAS, Prussian Blue, and Oil Red O staining show no enhanced carbohydrate, iron, or fat depositions in sections of Wls-HECKO livers in comparison to Ctrl. Scale bar = 100 μm; n = 7; 13-week-old males were used.
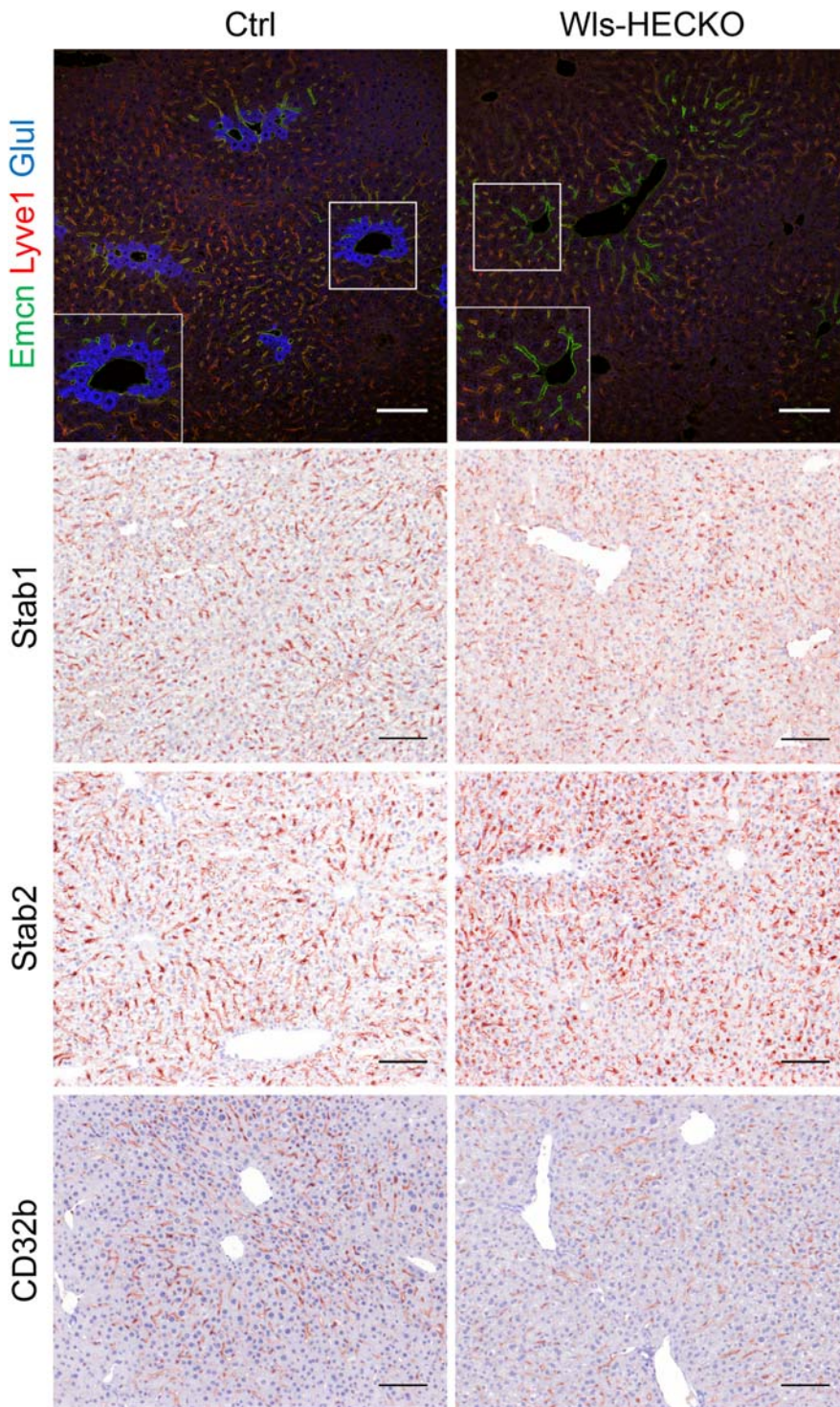
FIG. 5. HEC markers remain unchanged in Wls-HECKO. Representative pictures of immunofluorescence (20× objective) showing strong EMCN (green) staining in CVECs and pericentral LSECs; LYVE1 (red) is low in this area and highly positive in midlobular LSECs in both Ctrl (left) and Wls-HECKO (right). Glul (blue) is expressed in HCs adjacent to CVECs expressing EMCN in Ctrl (inset, left), whereas Glul is missing in Wls-HECKO (inset, right). Representative pictures of IHC (10× objective) for LSEC markers Stab1 and Stab2, which are expressed in all LSECs, whereas CD32b is stronger in midlobular LSECs. Wls-HECKO livers show a similar staining pattern to Ctrl for all markers. Scale bar = 100 μm; n = 5. Abbreviation: IHC, immunohistochemistry.

reach statistical significance ($P = 0.0759$; Fig. 1C). A reduced LW/BW in Wls-HECKO was observed in both male (4.1% in Wls-HECKO vs. 5.1% in control mice; $P < 0.01$) and female mice (3.1% in Wls-HECKO vs. 4.2% in control mice; $P < 0.01$; (Fig. 1D,E).

ANGIOCRINE Wnt SIGNALING CONTROLS METABOLIC LIVER ZONATION, BUT NOT HEC ZONATION IN THE HEPATIC LOBULE

Immunohistochemistry of marker proteins for metabolic liver zonation showed decreased expression of Glul, RhBg, and CYP2E1 characteristic for pericentral HCs in Wls-HECKO. Vice versa, Arg1 expression was extended in Wls-HECKO liver comprising pericentral HCs, which did not express Arg1 in control animals (Fig. 2). Co-IF of β-catenin with EMCN and zonation markers (Fig. 3A) showed a membranous β-catenin localization in control as well as Wls-HECKO livers, with no cytoplasmatic or nuclear β-catenin detectable in pericentral HCs. Upon *in situ* hybridization, strong Axin2 expression was observed in pericentral HCs in control mice, whereas it was almost absent in Wls-HECKO livers (Fig. 3B). No obvious alterations were detected in Wls-HECKO livers in comparison to control specimens upon H&E histology, PAS, or Sirius Red staining, indicating absence of liver fibrosis. Upon Prussian blue and Oil Red O staining, no alterations in iron deposition and lipid storage and distribution were detectable in Wls-HECKO as compared to control livers (Fig. 4). Additionally, Wls-HECKO did not exhibit significant changes of ALT, AST, GLDH, cholinesterase, and total protein in their plasma (Supporting Table S2). In contrast to the alterations in metabolic liver zonation, expression of zonal EC-specific markers EMCN and LYVE1 were not altered in Wls-HECKO in comparison to control livers; furthermore, a panel of LSEC differentiation markers, such as Stab1, Stab2, and CD32b, showed no differences in expression between Wls-HECKO and control livers (Fig. 5). In addition, transmission electron microscopy (TEM) did not show significant ultrastructural alterations in LSECs of Wls-HECKO (Supporting Fig. S5).

METABOLIC CHARACTERISTICS OF Wls-HECKO

Cholesterol levels were significantly reduced in plasma samples of both female and male Wls-HECKO mice in comparison to controls (Fig. 6A). Total cholesterol levels in liver lysates as well as expression of 3-hydroxy-3-methylglutaryl-coenzyme A reductase (HMGCR) and CYP7A1 were unaltered in Wls-HECKO mice (Fig. 6B and Supporting Fig. S6).

Sterole levels in plasma and liver lysates showed a trend toward lower levels in Wls-HECKO that did not reach statistical significance (Supporting Table S3A). Total acylcarnitines were elevated in blood samples from Wls-HECKO mice (Fig. 6C), but no significant differences were found regarding amino acid levels, including glutamine and arginine, as well as regarding single lipid metabolism intermediates (Supporting Table S3B). Plasma triglyceride levels (Fig. 6D) and basal blood glucose levels (Fig. 6E) were unaltered. Male Wls-HECKO displayed elevated bilirubin levels, whereas female Wls-HECKO plasma bilirubin levels did not reach statistical significance, in comparison to control animals, and hepatic heme oxygenase 1 (HMOX1) expression was increased in Wls-HECKO males (Fig. 6F). Plasma and hepatic total bile acid concentrations in plasma and liver showed a slight trend to higher values in Wls-HECKO that did not reach statistical significance (Supporting Table S3C). The ultrastructural morphology of bile canalicular structures (tight junctions, microvilli, and diameter) appeared unaltered on TEM (Supporting Fig. S7).

TRANSGENIC EXPRESSION OF C-TERMINALLY TAGGED Wls-YFP RESCUES LOSS OF FUNCTION OF Wls IN Wls-HECKO

Stab2-Cre$^{tg/wt}$;Wls$^{fl/fl}$;Rosa26:Wls-YFP$^{fl/wt}$ (Wls-rescue) showed expression of C-terminally tagged Wls-YFP fusion protein in HECs. In Wls-rescue, Co-IF of ICAM1 and YFP showed focal YFP staining in the perinuclear area of HECs (Fig. 7A). Wls-rescue showed RhBg (Fig. 7A) and Glul (Fig. 7B) expression in pericentral HCs similar to normal control livers (Fig. 7E,F), which was absent in Wls-HECKO;eYFP (Fig. 7C,D), indicating restoration of normal metabolic liver zonation. Zonal EC marker protein EMCN was expressed by CVECs and pericentral LSECs, whereas LSEC marker protein LYVE1 was expressed by midlobular LSECs in control, Wls-HECKO, and Wls-rescue livers (Fig. 7B,D,F).

Discussion

In the present study, we showed that HEC-derived Wnt ligands control liver growth and metabolic maturation. Angiocrine Wnt signaling maintains LW/BW in mice, suggesting that organotypic endothelium is a decisive regulator of organ size.[36,37] The Axin2$^+$,
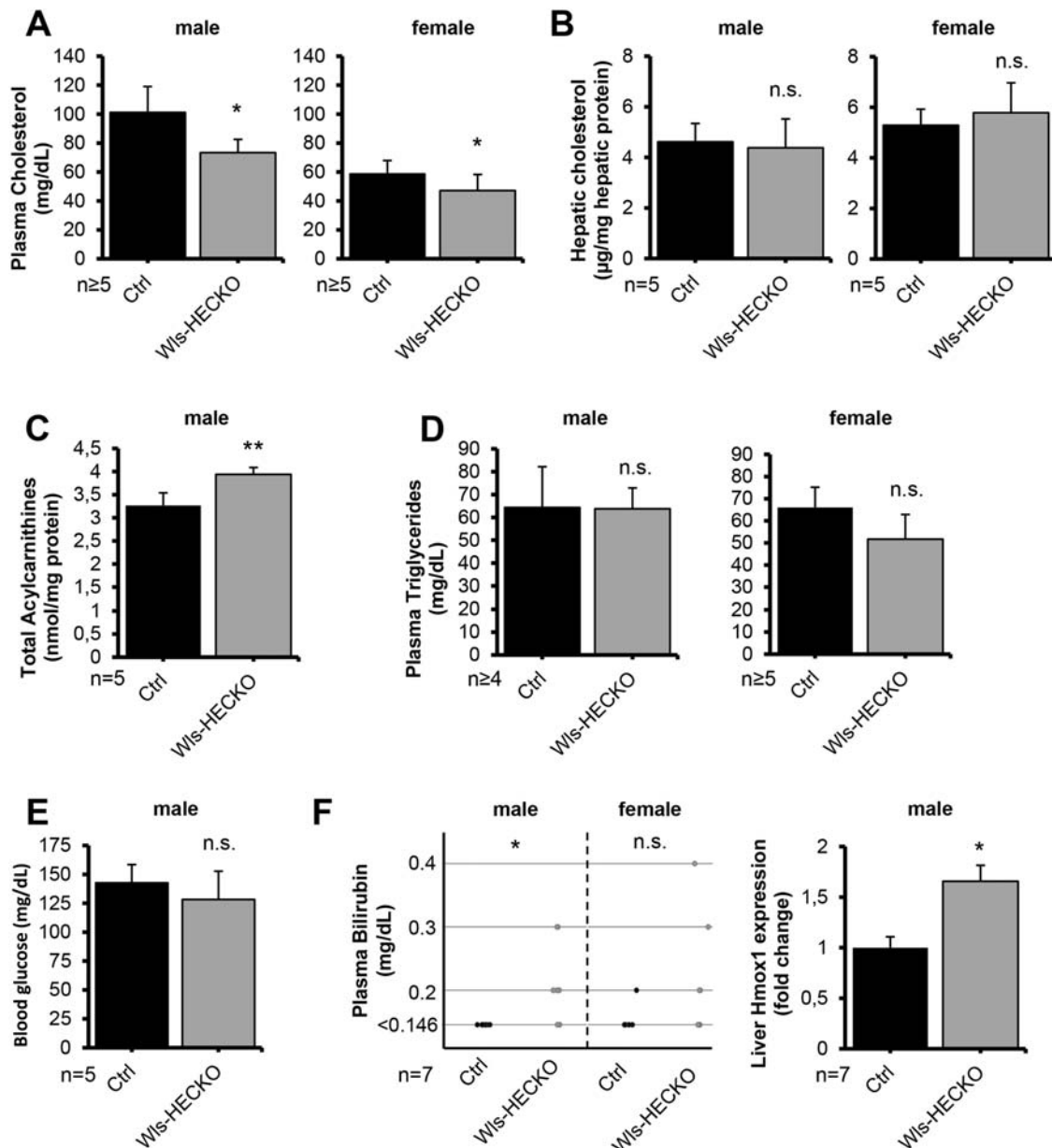
FIG. 6. Slightly altered fat metabolism in Wls-HECKO animals (11 weeks old; *$P < 0.05$; **$P < 0.01$; n.s. = not significant [$P > 0.05$]). (A) Plasma cholesterol is lower in both male (101 mg/dL in Ctrl vs. 73 mg/dL in Wls-HECKO) and female (59 mg/dL in Ctrl vs. 47 mg/dL in Wls-HECKO) Wls-HECKO mice. (B) Liver cholesterol did not differ significantly in both sexes. (C) Dry blood total acylcarnitines are significantly elevated in male Wls-HECKO mice (3.27 vs. 3.94 nmol/mg protein). (D) Plasma triglycerides remain unchanged in all subgroups. (E) Blood glucose in male mice does not differ significantly after 4 hours of fasting. (F) Left: Bilirubin levels exceed 0.145 mg/dL in male Wls-HECKO mice more often than in Ctrl; female mice showed no significance. Black dots represent single animal Ctrl, gray dots single animal Wls-HECKO bilirubin levels. Right: induction of hepatic HMOX1 shown by qRT-PCR. Fold change relative to β-Actin is shown; Ctrl was set to 1. Bars represent SEM. Mean fold induction in Wls-HECKO is 1.66 ($P = 0.0409$; n = 7).

Glul[+] HC subpopulation has been proposed to be part of the hepatic stem cell niche important for homeostatic renewal in the adult liver. Loss of this cell layer

suggests a correlation between lack of Wnt activation and reduction in liver size in Wls-HECKO mice.[13] Therefore, our data support the hypothesis that the
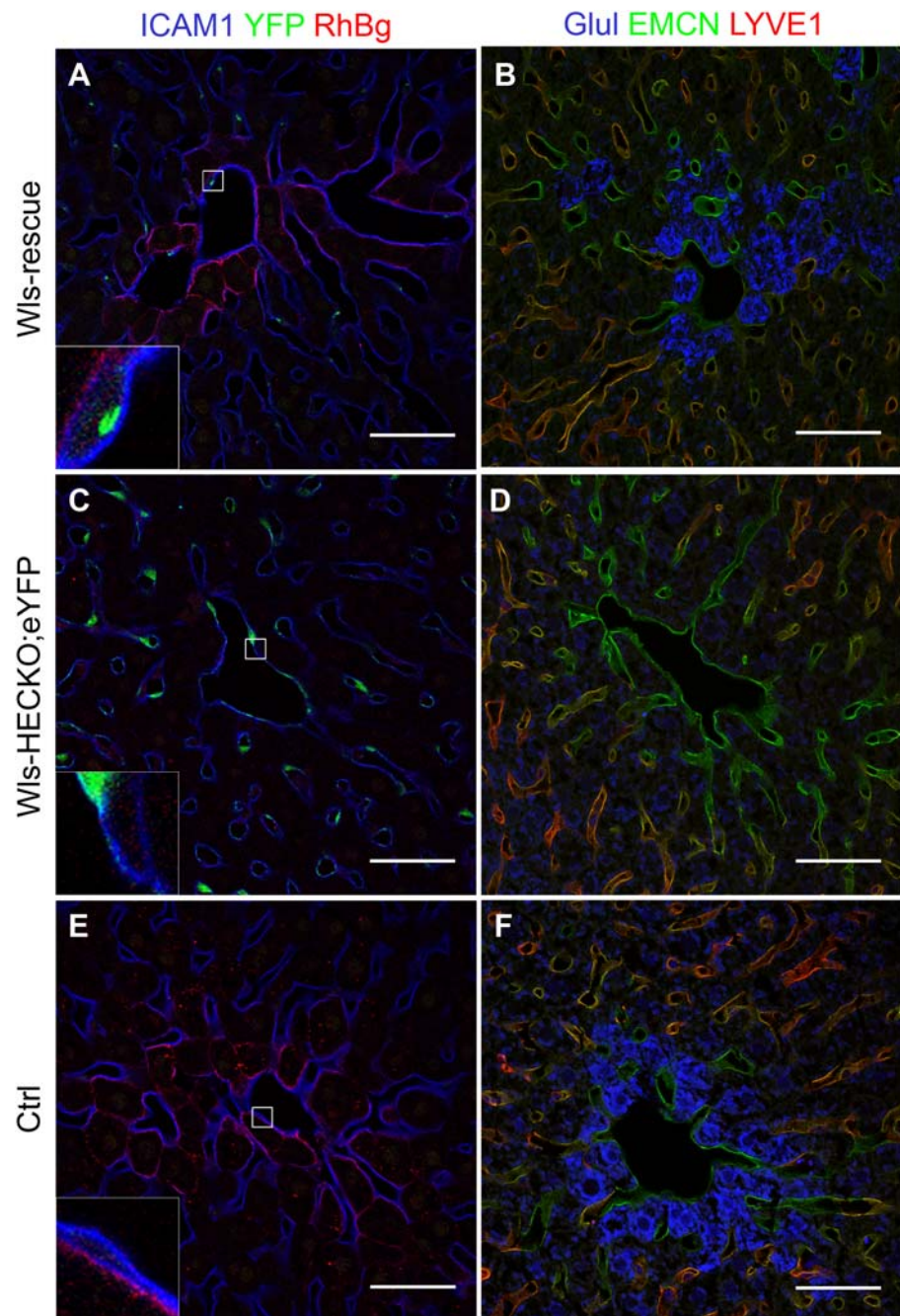
718

FIG. 7. RosaEvi-YFP expression in Wls-rescue livers. Representative pictures of immunofluorescence (63×objective) showing focal YFP (green) staining in HECs of Wls-rescue livers (A, n = 2), strong YFP staining in HECs of Wls-HECKO;eYFP (C, n = 5), and no YFP signal in Ctrl liver (E, n = 5). Ctrl (n = 5) and Wls-rescue (n = 2) livers show a pericentral, membranous RhBg staining pattern in HCs (A,E), which is absent in pericentral HCs in Wls-HECKO;eYFP (C). EMCN (green) staining is positive in CVECs and pericentral LSECs, whereas LYVE1 (red) is highly positive in midlobular LSECs of all groups (B,D,F). Glul (blue) is expressed in HCs adjacent to CVECs expressing EMCN in Wls-rescue (B) and Ctrl (F). Wls-HECKO;eYFP shows no signal for Glul. (F). Scale bar = 50 μm.

organ-specific vascular niche can indeed act as a rheostat for controlling the organ-specific parenchymal stem cell niche.[36]

Reduction of liver size in Wls-HECKO mice was accompanied not only by disruption of metabolic liver zonation, but also by alterations in lipid metabolism, including reduction of plasma cholesterol and elevation of total acylcarnitine blood levels that partially resemble mouse models of HC-specific loss of β-catenin signaling.[21,22,25,38] HC-associated liver dysfunction is not a likely cause of these metabolic changes given that Wls-HECKO mice showed neither liver fibrosis nor significant changes of ALT, AST, GLDH, cholinesterase activity, or protein synthesis. Notably, however, total acylcarnitine blood levels have been reported to be caused by increased beta-oxidation

during fasting.[39,40] Given that fasting has also been described to inhibit cholesterol synthesis,[41] reduced plasma cholesterol levels may similarly indicate a metabolic state in Wls-HECKO mice that may resemble fasting and could contribute to a lower body weight. Levels of plasma cholesterol were reduced in Wls-HECKO mice, although we did not find any changes in HMGCR expression and no pronounced deficiency in sterole intermediates, indicating absence of defects in specific steps in the cholesterol synthesis pathway. Similarly, cholesterol elimination was undisturbed as shown by unaltered CYP7A1 expression and plasma and liver bile acid levels. Up-regulation of HMOX1 in Wls-HECKO is in line with a similar up-regulation in HC-specific β-catenin KO mice and may explain elevated plasma bilirubin levels in both models.[22]

The slight metabolic changes described in our model might exacerbate upon challenging by malnutrition, as already demonstrated for mouse models of HC-specific loss of β-catenin.[22,38] An altered homeostatic metabolic state may also explain the lower body weight in male Wls-HECKO mice ($\sim$6.8% change in body weight), which is, at least partially, caused by the lower liver weight in comparison to control animals, accounting for 1.3% absolute loss in body weight in male Wls-HECKO mice. The change in body weight might be detectable only in males because of the greater change in LW/BW as well as in overall body weight as compared to female Wls-HECKO mice, in which the mean body weight difference did not reach statistical significance.

Notably, transgenic expression of YFP-tagged Wls protein restored metabolic liver zonation in Wls-rescue mice in comparison to Wls-HECKO. Previous studies had shown that expression of a C-terminally tagged Wls-V5, concomitant with small interfering RNA–mediated knockdown of WT Wls, mediated canonical Wnt signaling reporter activity.[42] Thus, Wls-HECKO mice could serve as an *in vivo* reporter system for tagged or altered Wls-construct functionality as well as other regulators of Wnt secretion routes. In this context, HC Glul and RhBg expression could serve as surrogate readout parameters for functional Wnt ligand exocytosis, whereas absence of these proteins would indicate disruption of angiocrine Wnt signaling.

Similar to Wls-HECKO mice, mice missing R-spondin receptors LGR4/5 in HCs show a significantly reduced LW/BW[24] and CVEC-derived RSPO3[23] has been shown to amplify Wnt-ligand-dependent activation of pericentral HCs. Thus, these data indicate that both angiocrine Wnt signaling and angiocrine R-spondin signaling are indispensable and interact in a nonredundant manner to maintain high-level canonical Wnt signaling in pericentral HCs and to guarantee a normal homeostatic LW/BW.

Given that expression of CYP2E1 and repression of E-Cadherin occur more than one HC layer distant from the central vein, it is an interesting question how midzonal HCs maintain low levels of β-catenin transcriptional activity.[43] In this respect, direct Wnt reporter expression analysis indicated that sustained Wnt signaling only occurs in one to three cell layers around the central vein.[44] A Wnt gradient originating from CVECs against the bloodstream seems highly unlikely; however, LSECs adjacent to the central vein may maintain low-level signaling through Wnt2. Transgenic mice expressing labeled Wnt ligands could help elucidate the exact mechanism of sustained angiocrine activation of canonical Wnt signaling in HCs. As an alternative, a recent single-cell RNA sequencing approach revealed a possible role of insulin-like growth factor signaling on HC differentiation in this area.[45]

Investigation of primary LSECs revealed that Wnt2 acts as an autocrine growth and differentiation factor in LSECs cross-stimulating vascular endothelial growth factor (VEGF) signaling,[14] and it has been demonstrated that VEGFA released from HCs is indispensable to maintain LSEC zonation and normal liver functions.[6] However, differentiation of pericentral and midlobular LSEC subsets seemed to be unaltered in Wls-HECKO as well as Wls-rescue mice, indicating that autocrine canonical as well as autocrine noncanonical Wnt signaling were dispensable for LSEC zonal differentiation. Differences in oxygen levels have been described as an additional novel mechanism guiding zonal HC differentiation,[45] with high oxygen levels in the periportal area and low oxygen levels in the pericentral region. Therefore, oxygen gradients might also play a role in LSEC spatial differentiation.

Angiocrine signaling from HECs to HCs is not only involved in guiding organ growth and metabolic functions in the liver, but also in liver regeneration, iron homeostasis, and angiogenesis.[9,11,13,23] Since endothelial dysfunction in macrovascular ECs is known to be an early step in the development of atherosclerosis,[46] less is known about endothelial dysfunction in microvascular ECs and its implication for disease pathogenesis.[47,48] Dysfunctional HECs have been reported to be involved in metabolic and cirrhotic liver disease as well as cancer.[49,50] Through altered

angiocrine signaling, dysfunctional HECs can induce pathological changes in other cells of the hepatic vascular niche, such as HCs, stellate cells, and macrophages. Therefore, HEC differentiation and multidirectional cross-talk between HECs and other cell types within the hepatic vascular niche in health and disease is a topic of high clinical significance, and elucidation of these processes will likely provide targets for therapeutic intervention.

REFERENCES

1) **Géraud C**, **Evdokimov K**, Straub BK, Peitsch WK, Demory A, Dorflinger Y, et al. Unique cell type-specific junctional complexes in vascular endothelium of human and rat liver sinusoids. PLoS One 2012;7:e34206.

2) **Géraud C**, **Koch PS**, **Zierow J**, Klapproth K, Busch K, Olsavszky V, et al. GATA4-dependent organ-specific endothelial differentiation controls liver development and embryonic hematopoiesis. J Clin Invest 2017;127:1099-1114.

3) **Schledzewski K**, **Géraud C**, Arnold B, Wang S, Grone HJ, Kempf T, et al. Deficiency of liver sinusoidal scavenger receptors stabilin-1 and -2 in mice causes glomerulofibrotic nephropathy via impaired hepatic clearance of noxious blood factors. J Clin Invest 2011;121:703-714.

4) Knolle PA, Wohlleber D. Immunological functions of liver sinusoidal endothelial cells. Cell Mol Immunol 2016;13:347-353.

5) Sorensen KK, Simon-Santamaria J, McCuskey RS, Smedsrod B. Liver sinusoidal endothelial cells. Compr Physiol 2015;5:1751-1774.

6) Walter TJ, Cast AE, Huppert KA, Huppert SS. Epithelial VEGF signaling is required in the mouse liver for proper sinusoid endothelial cell identity and hepatocyte zonation in vivo. Am J Physiol Gastrointest Liver Physiol 2014;306:G849-G862.

7) Mouta Carreira C, Nasser SM, di Tomaso E, Padera TP, Boucher Y, Tomarev SI, Jain RK. LYVE-1 is not restricted to the lymph vessels: expression in normal liver blood sinusoids and down-regulation in human liver cancer and cirrhosis. Cancer Res 2001;61:8079-8084.

8) Ding BS, Nolan DJ, Butler JM, James D, Babazadeh AO, Rosenwaks Z, et al. Inductive angiocrine signals from sinusoidal endothelium are required for liver regeneration. Nature 2010;468:310-315.

9) **Koch PS**, **Olsavszky V**, Ulbrich F, Sticht C, Demory A, Leibing T, et al. Angiocrine Bmp2 signaling in murine liver controls normal iron homeostasis. Blood 2017;129:415-419.

10) Canali S, Zumbrennen-Bullough KB, Core AB, Wang CY, Nairz M, Bouley R, et al. Endothelial cells produce bone morphogenetic protein 6 required for iron homeostasis in mice. Blood 2017;129:405-414.

11) **Hu J**, **Srivastava K**, Wieland M, Runge A, Mogler C, Besemfelder E, et al. Endothelial cell-derived angiopoietin-2 controls liver regeneration as a spatiotemporal rheostat. Science 2014;343:416-419.

12) **Ding BS**, **Cao Z**, Lis R, Nolan DJ, Guo P, Simons M, et al. Divergent angiocrine signals from vascular niche balance liver regeneration and fibrosis. Nature 2014;505:97-102.

13) Wang B, Zhao L, Fish M, Logan CY, Nusse R. Self-renewing diploid Axin2(+) cells fuel homeostatic renewal of the liver. Nature 2015;524:180-185.

14) Klein D, Demory A, Peyre F, Kroll J, Augustin HG, Helfrich W, et al. Wnt2 acts as a cell type-specific, autocrine growth factor in rat hepatic sinusoidal endothelial cells cross-stimulating the VEGF pathway. HEPATOLOGY 2008;47:1018-1031.

15) **Géraud C**, **Schledzewski K**, Demory A, Klein D, Kaus M, Peyre F, et al. Liver sinusoidal endothelium: a microenvironment-dependent differentiation program in rat including the novel junctional protein liver endothelial differentiation-associated protein-1. HEPATOLOGY 2010;52:313-326.

16) Bartscherer K, Pelte N, Ingelfinger D, Boutros M. Secretion of Wnt ligands requires Evi, a conserved transmembrane protein. Cell 2006;125:523-533.

17) Tan X, Behari J, Cieply B, Michalopoulos GK, Monga SP. Conditional deletion of beta-catenin reveals its role in liver growth and regeneration. Gastroenterology 2006;131:1561-1572.

18) Benhamouche S, Decaens T, Godard C, Chambrey R, Rickman DS, Moinard C, et al. Apc tumor suppressor gene is the "zonation-keeper" of mouse liver. Dev Cell 2006;10:759-770.

19) Gougelet A, Torre C, Veber P, Sartor C, Bachelot L, Denechaud PD, et al. T-cell factor 4 and beta-catenin chromatin occupancies pattern zonal liver metabolism in mice. HEPATOLOGY 2014;59:2344-2357.

20) Braeuning A, Ittrich C, Kohle C, Hailfinger S, Bonin M, Buchmann A, Schwarz M. Differential gene expression in periportal and perivenous mouse hepatocytes. FEBS J 2006;273:5051-5061.

21) Yang J, Mowry LE, Nejak-Bowen KN, Okabe H, Diegel CR, Lang RA, et al. beta-catenin signaling in murine liver zonation and regeneration: a Wnt-Wnt situation! HEPATOLOGY 2014;60:964-976.

22) Behari J, Yeh TH, Krauland L, Otruba W, Cieply B, Hauth B, et al. Liver-specific beta-catenin knockout mice exhibit defective bile acid and cholesterol homeostasis and increased susceptibility to diet-induced steatohepatitis. Am J Pathol 2010;176:744-753.

23) Rocha AS, Vidal V, Mertz M, Kendall TJ, Charlet A, Okamoto H, Schedl A. The Angiocrine Factor Rspondin3 Is a Key Determinant of Liver Zonation. Cell Rep 2015;13:1757-1764.

24) **Planas-Paz L**, **Orsini V**, Boulter L, Calabrese D, Pikiolek M, Nigsch F, et al. The RSPO-LGR4/5-ZNRF3/RNF43 module controls liver zonation and size. Nat Cell Biol 2016;18:467-479.

25) Liu H, Fergusson MM, Wu JJ, Rovira II, Liu J, Gavrilova O, et al. Wnt signaling regulates hepatic metabolism. Sci Signal 2011;4:ra6.

26) Srinivas S, Watanabe T, Lin CS, William CM, Tanabe Y, Jessell TM, Costantini F. Cre reporter strains produced by targeted insertion of EYFP and ECFP into the ROSA26 locus. BMC Dev Biol 2001;1:4.

27) Augustin I, Gross J, Baumann D, Korn C, Kerr G, Grigoryan T, et al. Loss of epidermal Evi/Wls results in a phenotype resembling psoriasiform dermatitis. J Exp Med 2013;210:1761-1777.

28) Augustin I, Goidts V, Bongers A, Kerr G, Vollert G, Radlwimmer B, et al. The Wnt secretion protein Evi/Gpr177 promotes glioma tumourigenesis. EMBO Mol Med 2012;4:38-51.

29) Schmelzer C, Okun JG, Haas D, Higuchi K, Sawashita J, Mori M, Doring F. The reduced form of coenzyme Q10 mediates distinct effects on cholesterol metabolism at the transcriptional and metabolite level in SAMP1 mice. IUBMB Life 2010;62:812-818.

30) Haas D, Morgenthaler J, Lacbawan F, Long B, Runz H, Garbade SF, et al. Abnormal sterol metabolism in holoprosencephaly: studies in cultured lymphoblasts. J Med Genet 2007;44:298-305.

31) Helenius A, Simons K. The binding of detergents to lipophilic and hydrophilic proteins. J Biol Chem 1972;247:3656-3661.

32) Rashed MS, Bucknall MP, Little D, Awad A, Jacob M, Alamoudi M, et al. Screening blood spots for inborn errors of metabolism by electrospray tandem mass spectrometry with a microplate batch process and a computer algorithm for automated flagging of abnormal profiles. Clin Chem 1997;43:1129-1141.

33) Schulze A, Kohlmueller D, Mayatepek E. Sensitivity of electrospray-tandem mass spectrometry using the phenylalanine/tyrosine-ratio for differential diagnosis of hyperphenylalaninemia in neonates. Clin Chim Acta 1999;283:15-20.

34) Okun JG, Kolker S, Schulze A, Kohlmuller D, Olgemoller K, Lindner M, et al. A method for quantitative acylcarnitine profiling in human skin fibroblasts using unlabelled palmitic acid: diagnosis of fatty acid oxidation disorders and differentiation between biochemical phenotypes of MCAD deficiency. Biochim Biophys Acta 2002;1584:91-98.

35) Diehl L, Schurich A, Grochtmann R, Hegenbarth S, Chen L, Knolle PA. Tolerogenic maturation of liver sinusoidal endothelial cells promotes B7-homolog 1-dependent CD8+ T cell tolerance. HEPATOLOGY 2008;47:296-305.

36) Rafii S, Butler JM, Ding BS. Angiocrine functions of organ-specific endothelial cells. Nature 2016;529:316-325.

37) Nolan DJ, Ginsberg M, Israely E, Palikuqi B, Poulos MG, James D, et al. Molecular signatures of tissue-specific microvascular endothelial cell heterogeneity in organ maintenance and regeneration. Dev Cell 2013;26:204-219.

38) Liu S, Yeh TH, Singh VP, Shiva S, Krauland L, Li H, et al. beta-catenin is essential for ethanol metabolism and protection against alcohol-mediated liver steatosis in mice. HEPATOLOGY 2012;55:931-940.

39) Costa CC, de Almeida IT, Jakobs C, Poll-The BT, Duran M. Dynamic changes of plasma acylcarnitine levels induced by fasting and sunflower oil challenge test in children. Pediatr Res 1999;46:440-444.

40) Reuter SE, Evans AM. Carnitine and acylcarnitines: pharmacokinetic, pharmacological and clinical aspects. Clin Pharmacokinet 2012;51:553-572.

41) Lorbek G, Lewinska M, Rozman D. Cytochrome P450s in the synthesis of cholesterol and bile acids—from mouse models to human diseases. FEBS J 2012;279:1516-1533.

42) Yu J, Chia J, Canning CA, Jones CM, Bard FA, Virshup DM. WLS retrograde transport to the endoplasmic reticulum during Wnt secretion. Dev Cell 2014;29:277-291.

43) Sekine S, Ogawa R, McManus MT, Kanai Y, Hebrok M. Dicer is required for proper liver zonation. J Pathol 2009;219:365-372.

44) Ferrer-Vaquer A, Piliszek A, Tian G, Aho RJ, Dufort D, Hadjantonakis AK. A sensitive and bright single-cell resolution live imaging reporter of Wnt/ss-catenin signaling in the mouse. BMC Dev Biol 2010;10:121.

45) Bahar Halpern K, Shenhav R, Matcovitch-Natan O, Toth B, Lemze D, Golan M, et al. Single-cell spatial reconstruction reveals global division of labour in the mammalian liver. Nature 2017;542:352-356.

46) Dharmashankar K, Widlansky ME. Vascular endothelial function and hypertension: insights and directions. Curr Hypertens Rep 2010;12:448-455.

47) Kanda T, Brown JD, Orasanu G, Vogel S, Gonzalez FJ, Sartoretto J, et al. PPARgamma in the endothelium regulates metabolic responses to high-fat diet in mice. J Clin Invest 2009;119:110-124.

48) Gimbrone MA, Jr., Garcia-Cardena G. Endothelial cell dysfunction and the pathobiology of atherosclerosis. Circ Res 2016;118:620-636.

49) Xie G, Wang X, Wang L, Wang L, Atkinson RD, Kanel GC, et al. Role of differentiation of liver sinusoidal endothelial cells in progression and regression of hepatic fibrosis in rats. Gastroenterology 2012;142:918-927.e6.

50) DeLeve LD. Liver sinusoidal endothelial cells in hepatic fibrosis. HEPATOLOGY 2015;61:1740-1746.

Author names in bold designate shared co-first authorship.

Supporting Information

Additional Supporting Information may be found at onlinelibrary.wiley.com/doi/10.1002/hep.29613/suppinfo.